

HOSTED BY



Contents lists available at ScienceDirect

Journal of King Saud University – Science

journal homepage: www.sciencedirect.com

Original article

Analyses of biosynthesized silver nanoparticles produced from strawberry fruit pomace extracts in terms of biocompatibility, cytotoxicity, antioxidant ability, photodegradation, and in-silico studies



Mahboob Alam

Department of Safety Engineering, Dongguk University, 123 Dongdae-ro, Gyeongju-si, Gyeongsangbuk-do 780-714, Republic of Korea

ARTICLE INFO

Article history:

Received 29 July 2022

Revised 31 August 2022

Accepted 14 September 2022

Available online 20 September 2022

Keywords:

Biogenic AgNPs

Biocompatibility

Cytotoxicity

Strawberry fruit pomace

In-silico study

ABSTRACT

Numerous disciplines, including biology and materials science, are using nanoparticle engineering. Silver nanoparticles (AgNPs) are produced from strawberry pomace extracts using cutting-edge technology. Biosynthesized nanoparticles were examined for their formation, shape, crystallinity, and size at the nanoscale using a variety of spectral techniques, such as UV-vis absorption spectra, X-ray powder diffraction (XRD), scanning, transmission electron microscopy (SEM/TEM), and their associated techniques like energy-dispersive X-ray (EDX or EDS), and selective area electron diffraction (SAED). AgNPs formation was observed by the surface plasmon resonance (SPR) observation at 431 nm, which was caused by the collective oscillation of the silver nanoparticles' free electrons. AgNPs were confirmed by EDX, showing a distribution of elements and having a distinct peak at 3.0 keV. Thermogravimetric analysis (TGA) was utilized to evaluate the thermal stability of NPs in a nitrogen atmosphere. Spectrophotometry was utilized to investigate the photocatalytic degradation of methyl orange employing biogenic NPs as nanocatalysts. The solution's decolonization revealed that the dye degrades gradually with longer exposure times. Antioxidant capability was evaluated using the stable free radical 2,2-Diphenyl-1-picrylhydrazyl (DPPH). Additionally, testing for biocompatibility and toxicity employing brine shrimps and red blood cells, respectively, revealed remarkable hemocompatibility with RBCs and no observable toxicity to brine shrimps at lower AgNPs concentrations. Additionally, the active amino acids involved in brine shrimp egg hatching were identified using molecular docking of silver nanoparticles against serine protease. Moreover, to look into non-bonding interactions with the amino acids of the enzyme that can inhibit cyst hatching and healthy growth of brine shrimp naupli.

© 2022 The Author(s). Published by Elsevier B.V. on behalf of King Saud University. This is an open access article under the CC BY-NC-ND license (<http://creativecommons.org/licenses/by-nc-nd/4.0/>).

1. Introduction

Nanotechnology is generating great enthusiasm due to the unique properties of matter at the nanoscale, which allow previously unimaginable tasks to be visualized (Nouailhat 2010, Dan 2020). For more than two decades, numerous works on nanosciences and nanotechnologies have been published within and at the interface of multiple scientific disciplines, including physics, chemistry, biology, engineering sciences, and humanities and social sciences (Tarafdar et al., 2013, Bayda et al., 2019). These have been and continue to be major challenges for scientists to develop many more important applications, such as lower cost electrode, biosensor, and catalyst for bacterial biotoxin elimination, in a controlled manner depending on the particle size, shape and crystalline nature (Khan et al., 2019). In general, nanoparticles are atoms and molecules agglomerated in a sphere with a diameter

Abbreviations: AgNPs, silver nanoparticles; DLS, dynamic light scattering; DPPH, 2,2-Diphenyl-1-picrylhydrazyl; EDS, energy-dispersive X-ray spectroscopy; EDX, energy-dispersive X-ray; FTIR, Fourier Transform infrared spectroscopy; NPs, nanoparticles; PDIs, polydispersity indices; SAED, selected area electron diffraction; SEM, scanning electron microscope; TGA, thermogravimetric analysis; TEM, transmission electron microscopy; UV-vis, ultraviolet-visible spectroscopy; XRD, X-ray Powder Diffraction.

E-mail addresses: mahboobchem@gmail.com

Peer review under responsibility of King Saud University.



Production and hosting by Elsevier

<https://doi.org/10.1016/j.jksus.2022.102327>

1018-3647/© 2022 The Author(s). Published by Elsevier B.V. on behalf of King Saud University.

This is an open access article under the CC BY-NC-ND license (<http://creativecommons.org/licenses/by-nc-nd/4.0/>).

between 1 and 100 nm and they are excellent candidates for applications in medicine, catalysis, electrochemistry, biotechnology, and trace-substance detection (Ali et al., 2016, Sharma et al., 2019). Nanoparticles (NPs) with diverse morphologies and sizes have been prepared using different synthetic methods. While these methods have improved NPs, there is still a need to understand better ways to make things (Pokrajac et al., 2021). Industry and business could use this technology to make better, cleaner, safer, and smarter products, such as home appliances, communication technology, medicine, transportation, and agriculture (Kargozar and Mozafari 2018, Pokrajac et al., 2022). Compared to NPs made chemically, Biomolecule-coated NPs have higher biocompatibility. The biocompatibility of bioinspired NPs opens up more options in biomedicine and related fields. Biomolecule-based methods result in the design of NPs with unique morphologies and sizes. For example, verticillium biomass was exposed to an aqueous solution containing Ag⁺ ions to produce AgNPs with sizes ranging from 12 to 25 nm (Mukherjee et al., 2001). Similarly, plant extracts such as leaves, roots, latex, seeds, stems, flowers and calyx have been used in the synthesis of nanoparticles and act as stabilizers as well as reducing agents (Mitchell et al., 2021). Plant extracts are preferred over microorganisms for the synthesis of nanoparticles because they do not require the complex process of maintaining cell cultures or biohazards and are simple to scale up. These resources contain astoundingly large amounts of these chemicals, which makes them a great source large-scale production (Nagesh et al., 2022, Vinodhini et al., 2022). Furthermore, a simple and fast method for producing metal nanoparticles based on thermal reduction of their complexes (Warad et al., 2014, Azam et al., 2017), has also been documented (Aazam and El-Said 2014) and thoroughly characterized using various spectroscopic methods. Nanoparticle research has led to more uses in biomedical sciences, such as diagnostics, drug delivery systems, cancer treatment, biosensing, bioimaging, and antimicrobial progress including purification of water. Strawberries are a popular horticultural product consumed globally due to their distinctive smell and excellent nutritional value. Most horticultural products, especially strawberries, are rich in antioxidants and phytochemicals, which have the function of slowing down human aging and reducing the incidence of diseases such as infections, problems about the immune system and cancer (Zhang et al., 2020). The significant antioxidant activity of strawberries is mainly due to vitamin C and polyphenol components, especially anthocyanins, ellagic acid derivatives and flavonols (Garcia-Viguera et al., 1998, Hong et al., 2018, Fitri and Fitriastuti, 2019, Fierascu et al., 2020).

The use of strawberry fruit pomace extracts as a reducing and stabilizing agent in the synthesis of AgNPs was investigated in light of the advantages of green synthesis over other techniques, as described in the literature in which strawberry fruit extract was used to synthesize silver nanoparticles (Umoren et al., 2017). It is noteworthy that this study demonstrated the effectiveness of biosynthesized nanoparticles as photocatalyst for the degradation of MO solution under visible light irradiation. In addition, well-characterized nanoparticles of silver derived from extract by FTIR, XRD, UV-vis, SEM, TEM and associated methodologies, as well as EDX and SAED, were used to assess antioxidant activity with DPPH. Moreover, the present study also aimed to explore the toxicity and biocompatibility of AgNPs as viable alternatives for biomedical and environmental applications due to their eco-friendly production.

2. Materials and methods

Materials, preparation of aqueous extracts from strawberry waste, green synthesis of silver nanoparticles, characterization of biogenic silver nanoparticles, in vitro biocompatibility and cyto-

toxicity effects on brine shrimp (*Artemia salina*), molecular docking, antioxidant activity and experimental design for photocatalytic activity were included in additional information under the experimental section (Farnsworth 1966, Markham 1988, Schneidman-Duhovny et al., 2005, Barros et al., 2007, Malagoli 2007, Li et al., 2012, Arulvasu et al., 2014, Kyrychenko et al., 2015, Shanmuganathan et al., 2018), to maintain the word limit according to the author's instructions.

3. Results and discussion

Analytical and spectroscopic techniques are used to characterize nanoparticles in terms of their nature, shape, size, distribution, stability or aggregation state, morphology, elemental content, and dispersity (Dawadi et al., 2021, Mughal et al., 2021). In order to characterize silver nanoparticle formation, some of the fundamental techniques frequently employed in the identification of nanoscale materials were used as given below.

3.1. Scanning electron microscopy (SEM) and transmission electron microscopy (TEM) analysis

The two most common types of electron microscopy used for assessing a sample's topographical/surface composition, internal structure, and crystal structure at the micro- and nano-level are scanning electron microscopy (SEM) and transmission electron microscopy (TEM). The morphology and structure of the phytosynthesized AgNPs were investigated using SEM and TEM. Fig. 1(a and b) show SEM and TEM images of Ag nanoparticles, respectively. The SEM micrograph (Fig. 1a) clearly shows agglomerated silver nanoparticles with a borderline diameter and wider particle dissemination. The agglomerates may have formed as a result of the drying process. The Ag nanoparticles are also shown in the TEM images (Fig. 1b) to be spherical, including irregular in shape, and to range in size from 10 to 20 nm. Energy dispersive X-ray (EDX) and selective electron diffraction (SAED), which are linked to SEM and TEM, respectively, and discussed under the section of sub-units in this study, were also used to investigate AgNPs.

3.2. UV-visible spectroscopy analysis

UV-vis spectroscopy was used to characterize the optical properties of silver nanoparticles produced through biosynthesis, which depend on NPs size and shape. The technology is also useful for monitoring the stability of nanoparticles based on their optical properties, as well as an indirect method for determining the reduction of silver nitrate to silver nanoparticles in aqueous solution. The production of silver nanoparticles was revealed by the solution's color changing from red to coffee. The NPs also have free electrons, which contribute to the formation of a surface plasmon resonance (SPR) band. A time-dependent evaluation of UV-Visible absorption spectra for biogenic NPs is performed to determine whether the absorbance and position of the SPR band are affected. It was found that the biosynthesis of NPs was at its optimal after 24 h. Furthermore, as time progresses, the absorption peak increases (Fig. 2). Peak patterns under similar conditions as reported in the literature were found to be nearly identical. In the absorbance spectra of the conjugated AgNPs, the characteristic absorbance peak of AgNPs, which was found at 431 nm, could be seen.

3.3. XRD and SAED analysis

XRD analysis provides detailed information about the shape, size, and orientation of the nanoparticles. The X-ray diffraction pattern of silver nanoparticles biosynthesized using strawberry fruit

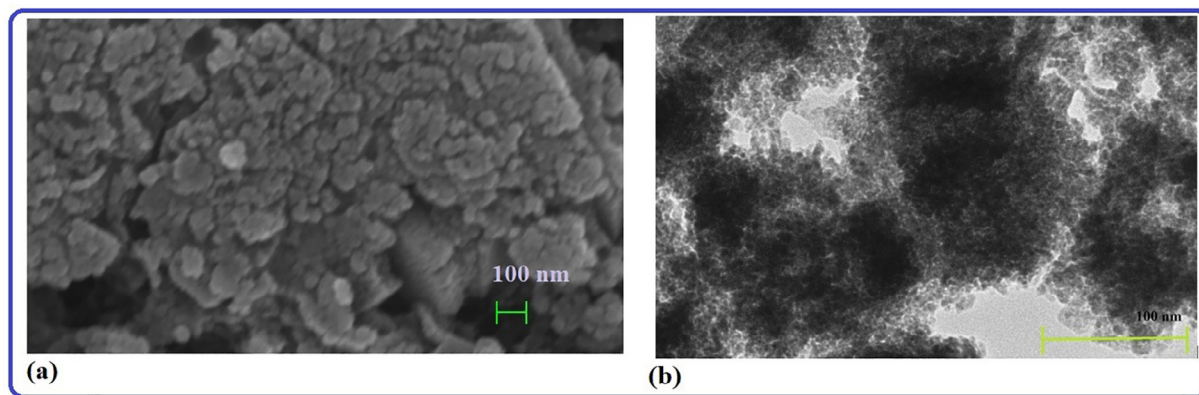


Fig. 1. (a) SEM and (b) TEM image of the biosynthesized AgNPs obtained from strawberry fruit pomace extracts.

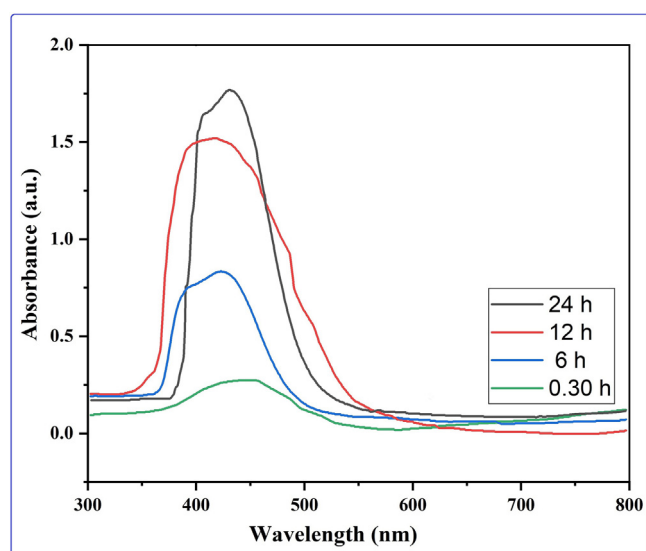


Fig. 2. Evaluation of the biogenic nanoparticles' UV-Visible absorption spectrum over a time span of about 30 min to 24 h.

waste material extract is shown in Fig. 3a with data collected for the 2θ range of 20 to 80° . Significant peaks in the XRD diffractogram at 2θ values of 38.32 , 44.41 , 64.53 , and 77.55° were discovered to be related to silver metal and correspond to (hkl) values (111) , (200) , (220) , and (311) planes of silver and are labeled in Fig. 3a. These patterns were compared to the diffractogram from JCPDS's standard powder diffraction card, silver file No. 04-0783. These reflections are in agreement with a silver metal that possesses face-centered cubic symmetry when compared to the JCPDS file. The high intensity peak of FCC materials appears as (111) reflection, indicating the high crystallinity of NPs. The diffraction peaks, however, are somewhat broad, indicating that the crystallite size is very small. In our study, the resultant particles were (FCC) Silver Nanoparticles. A peak at 32.32 deg, along with unmarked peaks, was also detected as being due to AgNO_3 , which could not be reduced or possibly the presence of Ag_2O in the biosynthesized Ag-nanoparticles, and these could represent the existence of some biogenic groups, which remained in trace levels in the sample. A prominent and intense peak at 2θ of 38.32° was chosen to compute crystal size using the Scherrer formula, $D = K\lambda/\beta \cos \theta$ (where K (customarily taken as 0.9), λ , β and θ stand for the Scherrer constant, the light's wavelength used for diffraction, the sharp peaks' full width at half maximum (FWHM), and the measured angle, respectively), which was found to be 11.57 nm. Moreover, the crystalline state of biogenic

AgNPs was determined using a selective area electron diffraction (SAED) pattern, as shown in Fig. 3b. SAED pattern displayed a variety of the set bright rings with spots as well as other rings resembling spheres and irregular shapes. The (111) , (200) , (220) , and (311) Bragg reflection planes (or hkl planes) were represented by these ring patterns (Fig. 3b). The brightest ring and the most intense peak in SAED and XRD patterns indicate that crystals are mostly oriented along the (111) Bragg reflection plane.

3.4. FTIR analysis

FTIR analysis of extracts and silver nanoparticles was used to investigate the significant functional groups in strawberry extract involved in the reduction of Ag^+ ions to Ag^0 , capping, and efficient stabilization of biosynthesized AgNPs (Fig. 4a and b). FTIR spectra of the biosynthesized nanoparticles as well extracts showed several major bands each of which suggested the presence of different functional groups of biomolecules present in extracts and its nanoparticles. The FTIR spectrum of strawberry fruit pomace extracts revealed a series of major absorption peaks in the wavelength ranges of 3864 – 3567 , 3033 , 2369 , 2322 , 1742 , 1699 , 1649 , 1540 , 1515 , 1034 , 842 , and 634 cm^{-1} , which can be assigned to $-\text{OH}$, $-\text{NH}$, aromatic $\text{C}-\text{H}$, $-\text{CN}$, various carbonyl groups with different environments, $\text{N}-\text{O}$, ether linkages including bending stretching, indicating various biomolecules. These absorption peaks in strawberry fruit extracts (Fig. 4a) detected flavonols, anthocyanins, flavanols, gallotannins, ellagitannins, hydroxycinnamic acids, hydroxybenzoic acids, proanthocyanidins, and other biomolecules (García-Viguera et al., 1998, Hong et al., 2018, Fitri and Fitriastuti, 2019, Fierascu et al., 2020). Similarly, the FTIR spectrum (Fig. 4b) of extract-derived biogenic silver nanoparticles revealed significant absorption peaks at 3307 , 2939 , 1722 , 1628 , 1345 , 1228 , 1035 , 822 , and 553 cm^{-1} , indicating the presence of OH functionality with broad band, $\text{C}-\text{H}$ band with asymmetric stretching vibration, $\text{C}=\text{O}$ carbonyl group stretching frequency, $\text{C}=\text{C}$ aromatic stretching, and aromatic amines. Another notable peak at 1016 cm^{-1} corresponds to an ester's $\text{C}-\text{O}$ stretching frequency, as well as some weak absorption peaks related to aromatic functionality. Phytochemicals noticeable in the IR spectrum act as reducing or capping agents for the fabrication of AgNPs. These phytochemicals found in aqueous extracts were then qualitatively tested in order to identify biochemical active compounds by observing the color change reaction that occurred when a specific reagent was added. These biochemical compounds, such as coumarins, saponins, tannin, flavonoids, volatile oils, sterols, and phenols, were identified using standard biochemical protocols (Farnsworth 1966).

Based on the foregoing discussion based on IR spectra, phytochemical analysis, HPLC-ESI-MS as well as literature (Karaaslan

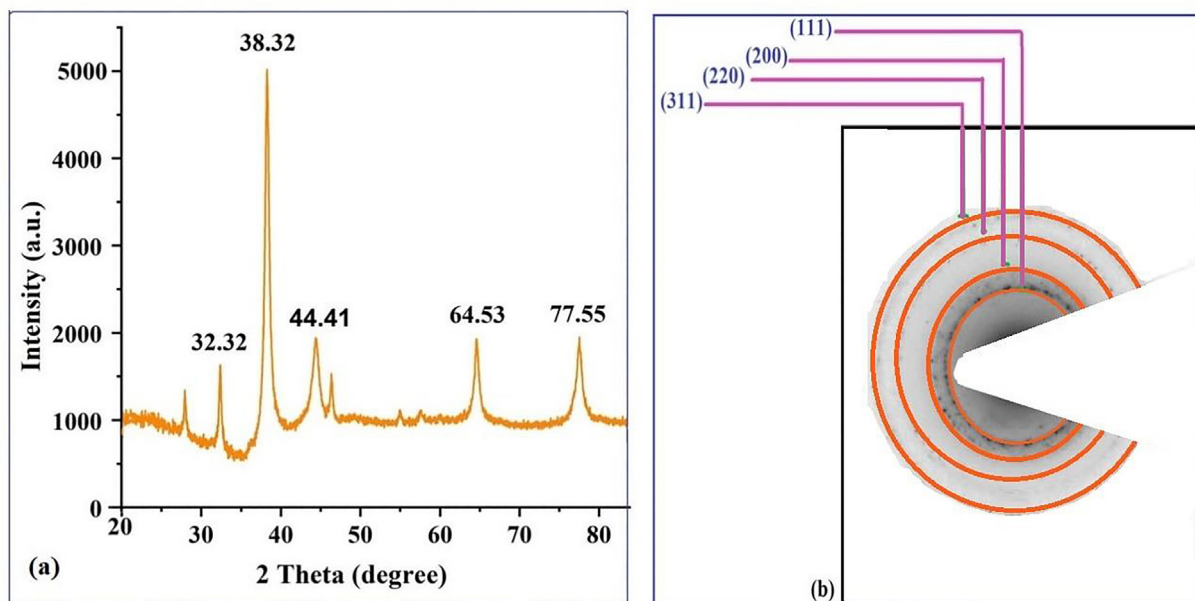


Fig. 3. (a) XRD pattern and (b) SAED pattern of the biogenic AgNPs with rings labeled.

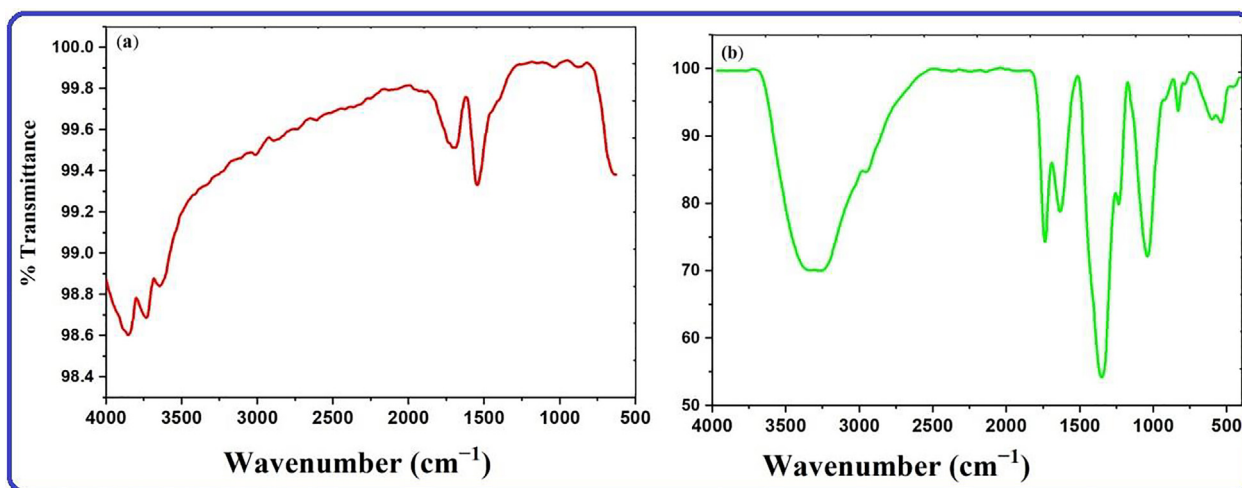


Fig. 4. FTIR of (a) extracts and (b) biogenic AgNPs.

and Yaman 2017, Guan et al., 2019, Unal et al., 2020), tentative mechanisms can be sketched to unravel the involvement of biomolecules for the production of nanoparticles, as shown below (Fig. 5). The chemistry of reducing metals or metal oxide nanoparticles is not the only factor influencing biomolecule involvement. Other factors, however, are at work during the biogenic synthesis of nanoparticles. In this process, silver ions (Ag^+) can capture electrons released by acid hydroxyl groups of biomolecules in extracts, specifically anthocyanins (flavonoid class), phenols, and ascorbic acid, to produce intermediate and convert them to silver (Ag^0) in extract solution, with phytomolecules acting as both capping and stabilizing agents.

3.5 Elemental dispersive spectrum and thermogravimetric analysis (TGA)

The energy dispersive spectroscopy (EDS) method was used to carry out qualitative analyses of chemical compositions in micro and nanoparticle samples, though it is capable of providing semi-

quantitative results. The EXD (or EDS) analysis in the Fig. 6a, which displayed varying intensities of signals at the X-axis of the various binding energies (keV), demonstrated the existence of different elements in the sample. A strong signal at 3 keV revealed the presence of metallic silver in silver nanoparticles biosynthesized using extracts. A peak in the XRD pattern at 32.32° , which corresponds to the other metallic silver in the EDX profile, indicates the existence of Ag_2O in the AgNPs sample (Roy et al., 2015, Jemal et al., 2017). Other weak to moderate signals were found in addition to the aforementioned signals. These included the presence of oxygen and carbon as a result of the preparation of the sample using a copper grid coated with carbon as well as the presence of carbon as a result of capping biomolecules. Fig. 6b of the EDX spectrum showed the elemental composition present except silver nanoparticles in sample. The spectrum showed that silver, constituting 53.29 % of the total, was the most important element, followed by carbon (33.5 %) and oxygen (13.21 %), demonstrating the formation of AgNPs.

Thermogravimetric analysis (TGA), in which the temperature-assisted decomposition behavior of biomolecule-coated nanoparti-

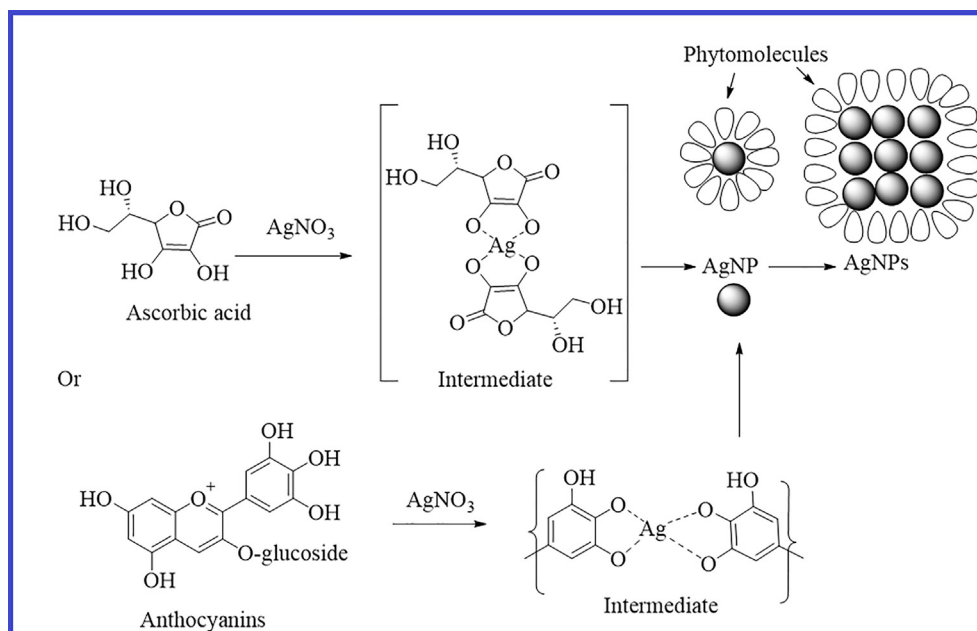


Fig. 5. Sketch of a possible mechanism for the formation of NPs and the involvement of an expected biomolecule (other biomolecules may be involved).

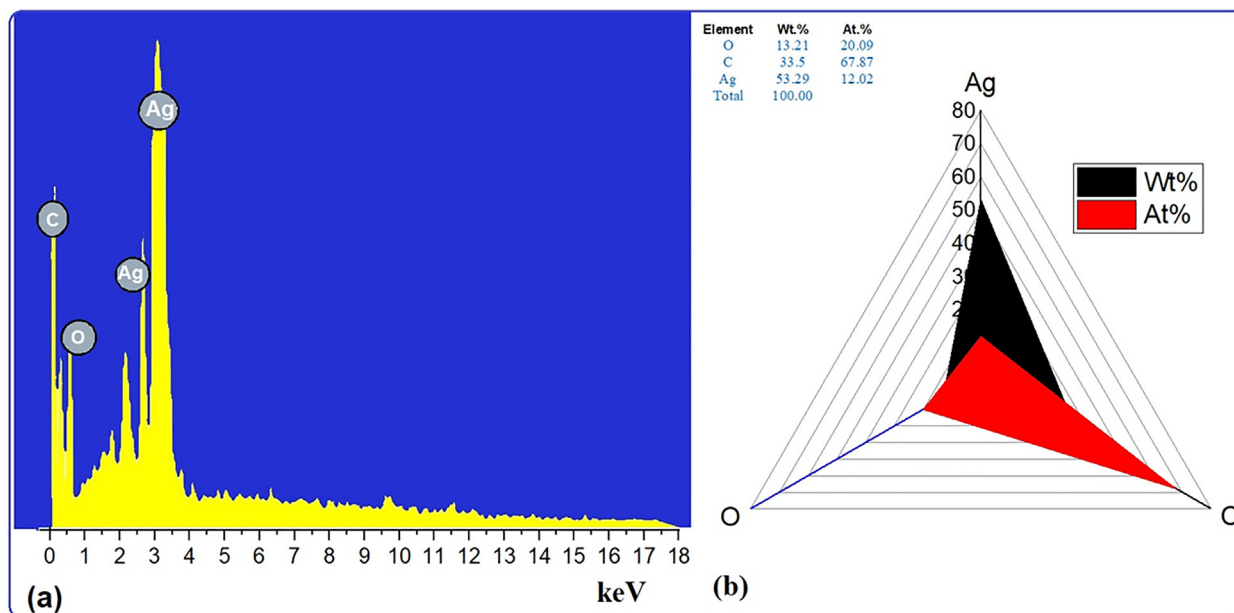


Fig. 6. (a) EDX images and (b) weight % of elements.

cles was explored, was used to examine the thermal stability of AgNPs produced by biosynthesis using aqueous extracts. Level of purity as well organic moieties capping the nanoparticles on their surface was estimated to calculate weight loss with temperature by TGA (Fig. 7a). There were certain phases of the weight loss process that were observed. About 2.5 % of the weight loss below 125 °C in the first stage is attributed to the physisorbed water or moisture content evaporating on the AgNP surface. The second, roughly 13 percent weight loss occurs in the temperature range of 125–500 °C and may be caused by the desorption or degradation of a variety of stable and unstable bioactive compounds, including phenols, proteins, and ellagic acid, which has a melting point of 350 °C and these bioactive compounds have been reported to be found in the strawberry fruit extract. The nanoparticles start to stabilize at >500, the last step, after a slight loss. The nanoparticles

still possessed approximately 75.0 % by weight with their stability and purity, according to the TGA.

3.6. Particles size and zeta potential analysis

Dynamic light scattering (DLS) is one of the most accessible physics methods for assessing the size and size distribution of NPs when a light source is employed to irradiate a colloidal solution. DLS for particle size can be performed using Brownian motion theory to measure the hydrodynamic diameter, which provides information about the metal or metal oxide core, as well as any coating material and the solvent layer attached to the particle. Similarly, biogenic nanoparticles with layers of biomolecules, including the solvent layer as it moves under Brownian motion, yield apparent particle size or hydrodynamic diameter. As shown in

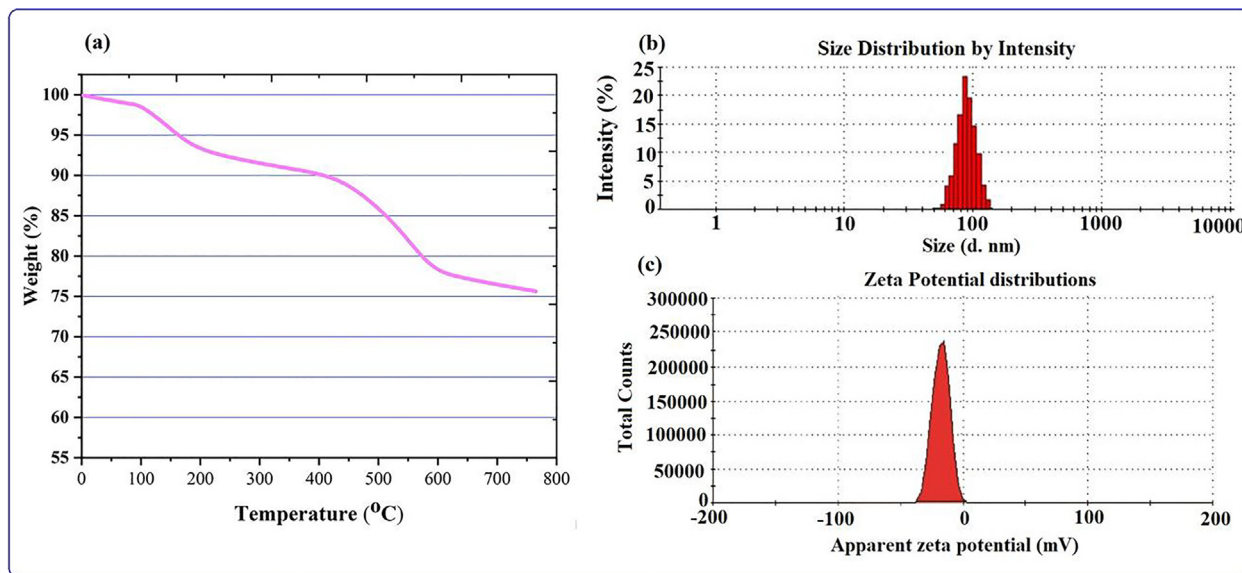


Fig. 7. (a) TGA (b) DLS and (c) zeta potential analysis of the biogenic NPs.

the Fig. 7b, the average size distribution of biogenic AgNPs was 85 ± 1.012 nm with polydispersity indices (PDIs) of 0.307 ± 0.008 . The polydispersity indices (PDIs) calculated for the extract-based biosynthesized are 0.307 ± 0.006 , which is within the range of 0–1 (Murdock et al., 2008), where 0 denotes monodisperse and 1 denotes polydisperse. The estimated PDI values clearly suggest that the majority of AgNP production occurred in the monodisperse phase, with minor amounts occurring in the polydisperse phase, and particle aggregations are also minimal. However, the average size of biosynthesized AgNPs is greater than in TEM studies because DLS measures the size of nanoparticles that are surrounding biomolecules with solvent layers in clusters. The Zeta potential (Fig. 7c) of the biogenic silver nanoparticle was investigated to find out more about the surface characteristics with charge distribution and the cessation of nanoparticle aggregation. The negative Zeta Potential of silver nanoparticles represents not the surface charge, but the net charge surrounding the particle under the electric field in solution. The AgNPs zeta potential value is seen in the Fig. 7c. The distribution of a particle is strongly influenced by the charge surrounding surface. Zeta potential for AgNPs was found to range from -4.16 to -37.5 mV. The presence of bioactive substances, such as polyphenolic compounds, on the surface of the AgNPs may be the cause of their negative charge. This suggests that there existed a repelling force between the AgNPs and that they were effectively segregated and stable throughout time. Particles with high zeta potential are repulsed by each other, which prevents them from aggregating (Priyadarshini et al., 2013, Moldovan et al., 2016).

3.7. Analysis of in vitro biocompatibility and cytotoxicity of NPs

The biocompatibility of biogenic nanoparticles was checked by testing their ability to break down red blood cells (RBCs). In this bioassay, the absorbance of RBCs at 570 nm was measured with a spectrophotometer to find out how much hemolysis was caused by different concentrations of AgNPs (3.125–500 $\mu\text{g}/\text{mL}$). The ability of a sample to rupture cells is necessary to detect red blood cell hemolysis. The American Society for Testing Materials defines compounds with >2 % hemolysis as nonhemolytic, compounds with 2–5 % hemolysis as slightly hemolytic, and compounds with >5 % hemolysis as hemolytic. This test was done with different amounts of silver nanoparticles, as shown in the Fig. 8a of the

biocompatibility (hem-compatible) results. The Fig. 8a shows the percentage of hemolysis of different concentrations of biological nanoparticles, and it was found that the hemolysis of RBCs increased with increasing NP concentration. At 25 and 100 $\mu\text{g}/\text{mL}$ biogenic NP, the lowest and maximum hemolysis in the systematic study were recorded at 3.3 % and 35.9 %, respectively (Fig. 8(A(a))). In short, it was established that the biogenic AgNPs produced from strawberry pomace extracts at a concentration of 50 $\mu\text{g}/\text{mL}$ under the ASTM E2524-08 standard were safe. The extent of the hemolysis that takes place has been shown to have a direct correlation with the average size of the NPs that were found in the literature (Chen et al., 2015).Fig. 9.

The marine crustacean *Artemia nauplii* was utilized for the purpose of determining the eco-toxicity assessments of AgNPs. The Fig. 8(A(b)) shows dose-dependent experiments in which dead brine shrimp were counted in experimental wells at nanoparticle concentrations ranging from 3.125 to 500 $\mu\text{g}/\text{mL}$ after 24 h of exposure without supply food. The mortality percentages for dosages of 0 (no NP), 3.15, 6.25, 12.5, 25, 50, 100, 200, 400, and 500 $\mu\text{g}/\text{mL}$ of AgNPs were 0, 0, 10, 20, 35, 50, 60 and 80, respectively. In the experimental data, a maximum mortality value of 80 ± 1.7 was found at 500 $\mu\text{g}/\text{mL}$ (similar to that described in literature (Faisal et al., 2021), while the lowest mortality value was found at 6.25 $\mu\text{g}/\text{mL}$. Metallic NPs have a dose-dependent toxicity pattern for *Artemia salina* based on findings in our study. AgNPs primarily cause death at high concentrations, making them ecotoxic. The literature and our study indicate that increased levels of AgNPs in the body lead to increased mortality, apoptotic cells, DNA damage, and gut clumping. The NPs themselves, as well as their breakdown products and NP agglomerates formed during the experiment, can all be toxic. On the basis of standards from the Organization for Economic Cooperation and Development (OECD), NPs can be summarized and classified as low-toxicity agents. It is nevertheless important for NPs to be considered appropriately for their ecological and environmental health consequences, based on the results of cytotoxicity assays.

3.8. Molecular docking analysis

Molecular docking was performed to find proper orientation and non-bonding interactions of the silver nanoparticles with enzymes named serine proteases for stable complex formation.

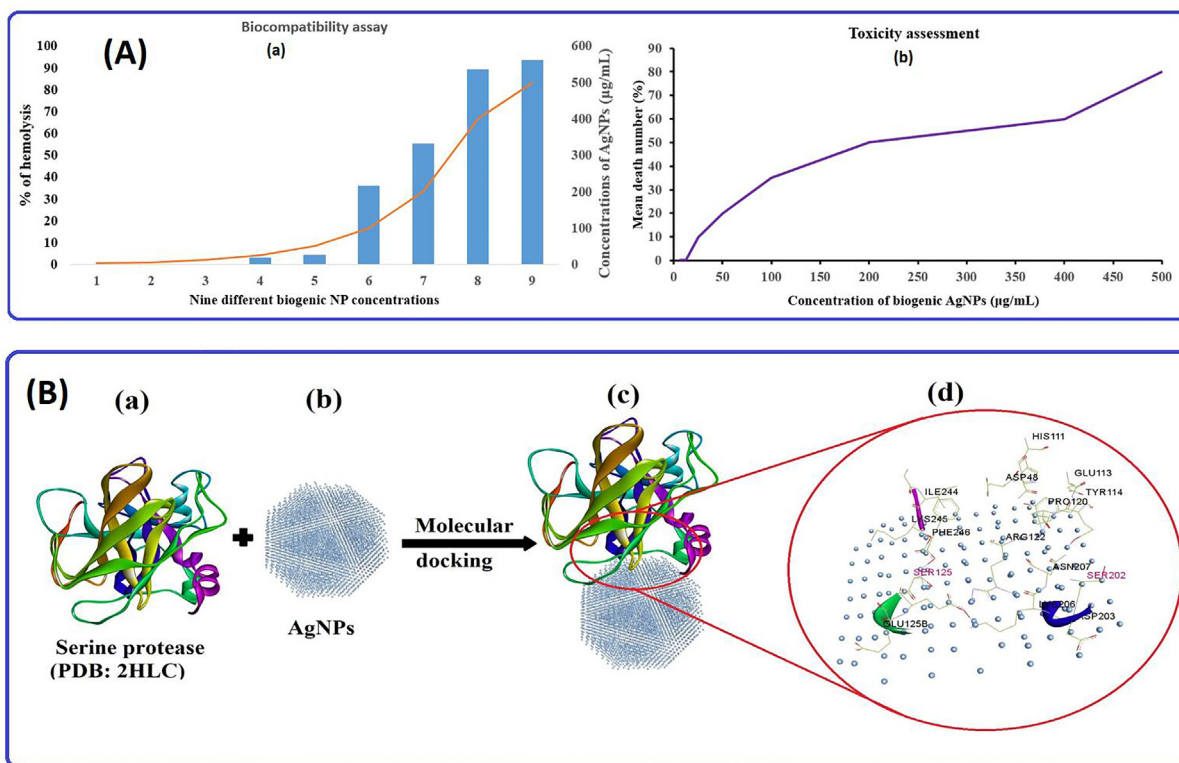


Fig. 8. (A(a)) % hemolysis behavior of biogenic AgNPs at different concentrations and (A(b)) correlation between AgNPs concentration and % mean mortality of brine shrimp for cytotoxicity assessment; (B) Molecular docking binding pattern analysis of (B(a)) serine protease; receptor with (B(b)) AgNPs, (B(c)) best possible docking pose, and (B(d)) various interactions of active amino acids, including SER in red and other amino acids of serine protease.

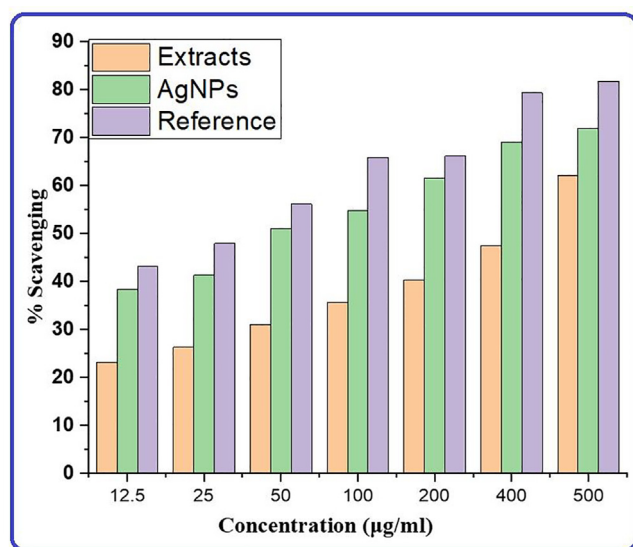


Fig. 9. Different colors show the antioxidant power of strawberry fruit pomace extracts, their silver nanoparticles, and a reference.

This enzyme was reported to act as a hatching enzyme in *A. salina* (Fan et al., 2010). Computational NPs-target binding approach was applied to investigate the possibility of inhibiting the hatching enzyme, serine protease, and to analyze the structural complexes of AgNPs with the enzyme to gain an understanding of its structural basis interaction (Fig. 8B). The best docking result with the binding energy of the model of -5.55 Kcal/mol was chosen, displaying non-binding interactions with key amino acids such as

HIS 111, ASP48, ASN49, GLU113, TYR114, GLN119, PRO120, ARG122, SER125, GLU126, SER202, ASN207, ASP203, LYS206, GLY243, ILE244, PHE246 and LYS2. The interaction of AgNPs with SER, HIS, and ASP, which play important roles in the cleaving ability of the proteases, inhibited hatching and nauplii growth.

3.9. Antioxidant analysis

As a consequence of free radical production by countless processes in the living system, as well as ultraviolet radiation generated by various chemical and physical processes in the environment, DNA, proteins, and lipids degraded. In such cases, the protection of biological systems requires the use of external antioxidants, as these play a critical part in their defense. To assess the antioxidant capacity of extracts and their biogenic silver nanoparticles, DPPH was used to perform free radical scavenging activity in percentage as shown in the Fig. 10. The extent of absorbance of the de-colorization of DPPH was used to measure the antioxidant activity of extracts and nanoparticles at varied concentrations. The capacity of radical scavenging was dosage dependent and increased with NPs concentration. Strawberry waste material (pomace) extracts and AgNPs exhibited maximum scavenging activities of 55.1 and 71.9 %, respectively, at $500\mu\text{g mL}^{-1}$ concentration and these data were compared to the reference and found in the following order: Reference > AgNPs > Extracts as represented in Fig. 10. Therefore, bio-silver nanoparticles exhibit greater scavenging activity than their extracts and can be used as an effective antioxidant agent due to the large surface area and capping of bioactive molecules on the surface of nanoparticles increase the antioxidant potential of NPs. Fruit extract supported nanoparticles are natural antioxidants that are effective for health protection against various oxidative stress associated with degenerative dis-

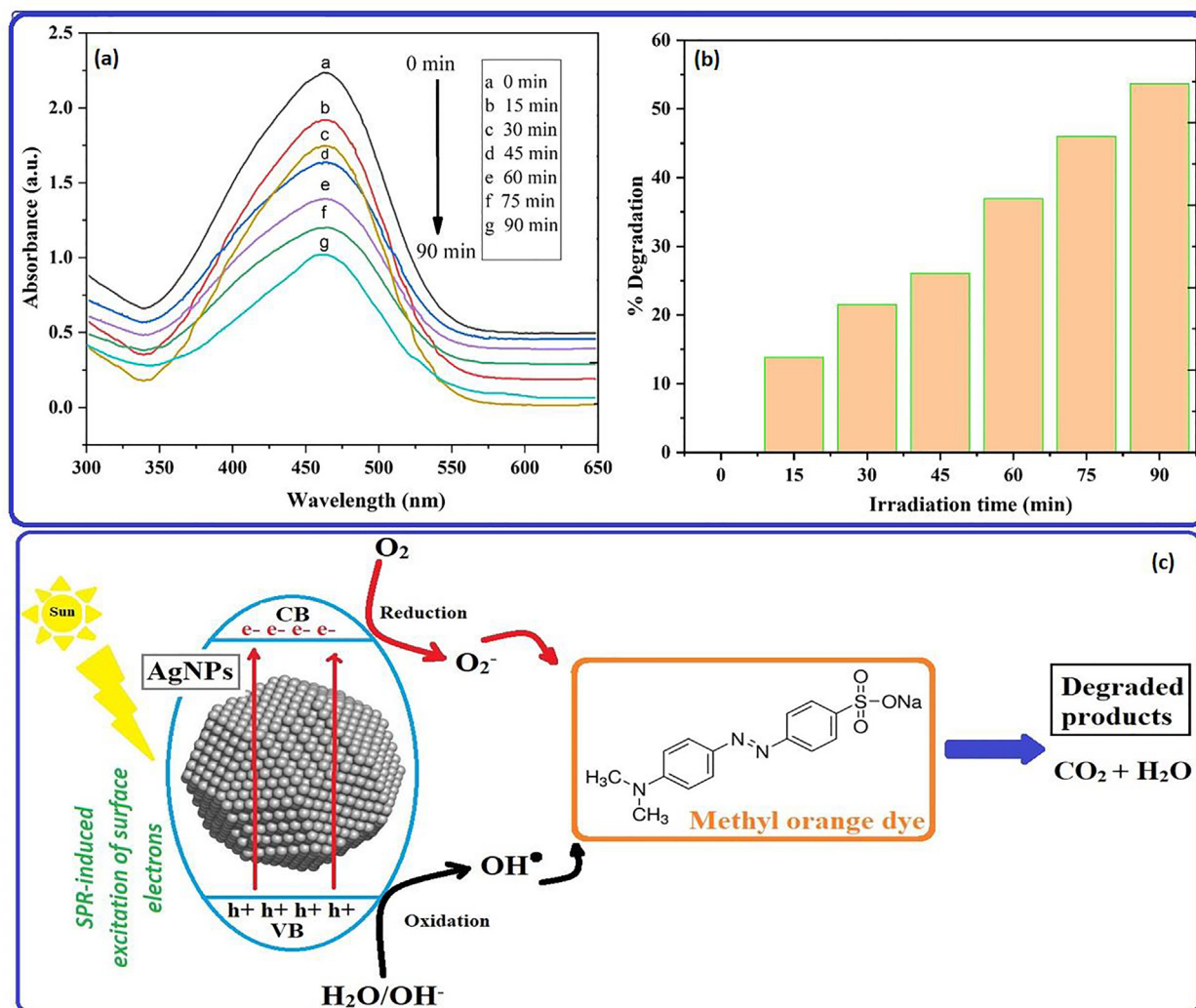


Fig. 10. (a) The intensity of the absorbance peak was observed to decrease as irradiation time duration was increased with NPs in the absorption spectra of MO dye and degradation efficiency, (b) % degradation vs irradiation time bar graph and (c) a photocatalytic trigger for dye degradation in the presence of AgNPs under direct sunlight exposure.

eases, and are of interest in the biosynthesis of new, safer antioxidants with minimal side effects.

3.10. Analysis of photocatalytic degradation activity

In the presence of biogenic nanoparticles, the photodegradation of the methyl orange (MO) dye was examined under visible light. Then, over the period of 90 min, the UV-vis spectrophotometer was used to measure the amount of photodegradation in terms of the absorbance of the MO solution at roughly 464 nm at specified intervals. In this experiment, the rate of degradation as a measure of the percentage of decolonization over time was measured after the methyl orange dye with a catalyst was swirled in the dark and exposed to sunlight. The Fig. 11, which illustrate the findings of the degradation studies, show that MO degradation rises with increasing irradiation time (Fig. 11a). It is evident from the absorbance spectra of MO (Fig. 11) that in the presence of biosynthesized nanoparticles, MO solution was degraded by 13.79, 21.49, 26.03, 36.91, 45.98, and 53.25 % after 15, 30, 24, 60, 75, and 90 min, respectively, as seen in the bar graph in Fig. 11b. It was observed that the MO dye degraded over time, and that the rate of degeneration increased with longer exposure times. Graphical representation (Fig. 11c) of the degradation of methyl orange uses

a preliminary mechanistic approach based on literature and is believed to be responsible for the simultaneous generation of electron-hole pairs in conduction and valence bands (VBs) on the photocatalyst AgNPs surface in response to light irradiation. Free holes and electrons in the valence and conduction band bands are used in redox processes with H₂O and O₂ molecules to produce OH radicals and O₂ superoxide radicals, respectively. As shown in a schematic diagram, absorption of sunlight by the surface of biogenic AgNPs can easily stimulate the migration of electrons and positive hole, thereby increasing the efficiency of degradation. The hydroxyl radicals produced at VBs and CBs function as strong oxidizing agents, degrading MO dye into simple inorganic molecules such as water, carbon dioxide, and inorganic ions.

4. Conclusions

Silver nanoparticles, in this paper, was fabricated using aqueous strawberry fruit pomace extracts as reducing and capping agents by cutting-edge technology of green synthesis. The morphology, crystallinity, size, and stability of benign silver nanoparticles was characterized applying different technology including UV-vis, XRD, SEM, TEM, EDX, SAED, DLS, zeta potential and TGA. The presence of biomolecules that were active in reducing silver ions to sil-

ver atoms was confirmed using FTIR and reagents of phytochemical analysis. The fabricated silver NPs have a face-centered cubic structure with a crystallite size of about 12 nm, as shown by the XRD patterns of the prepared NPs. The TEM image of the NPs shows spherical and irregular shapes in the size range of around 10–20 nm, however DLS revealed particles of about 85 nm, which are larger than in TEM analysis because DLS measures the size of nanoparticles that are clustered around biomolecules and have solvent layers on them. A radical scavenging (DPPH) experiment was used to study and compare the antioxidant capacity of aqueous extracts and biogenic AgNPs with a reference drug. Results showed the following pattern: reference > biogenic AgNPs > extracts. The biogenic of silver nanoparticles was used to assess cytotoxicity and biocompatibility for alternative uses in biological studies and was shown to be non-toxic and biocompatible at lower concentrations of NPs. Molecular docking of AgNPs against serine proteases was performed to examine nonbonding interactions of active amino acids in order to obtain information of the suppressing brine shrimp egg hatching. The fabricated silver nanoparticles were used to analyze the degradation and mechanism of methyl red dye and were reported to have stronger photocatalytic action, with approximately 53.25 percent degradation of MO with 90 min exposure lengths of time. Based on our findings, biogenic silver nanoparticles made from strawberry fruit pomace extracts rich in bioactive molecules could be used as convincing visible-light-driven photocatalyst for environmental remediation as well as in the healthcare domain for a variety of biological applications in the near future.

Declaration of Competing Interest

The authors declare that they have no known competing financial interests or personal relationships that could have appeared to influence the work reported in this paper.

Appendix A. Supplementary data

Supplementary data to this article can be found online at <https://doi.org/10.1016/j.jksus.2022.102327>.

References

- Aazam, E.S., El-Said, W.A., 2014. Synthesis of copper/nickel nanoparticles using newly synthesized Schiff-base metals complexes and their cytotoxicity/catalytic activities. *Biorganic Chemistry*. 57, 5–12.
- Ali, A., Zafar, H., Zia, M., et al., 2016. Synthesis, characterization, applications, and challenges of iron oxide nanoparticles. 9 49.
- Arulvasu, C., Jennifer, S.M., Prabhu, D., Chandhirasekar, D., 2014. Toxicity Effect of Silver Nanoparticles in Brine Shrimp *Artemia*. *The Scientific World Journal* 2014, 1–10.
- Azam, M., Dwivedi, S., Al-Resayes, S.I., et al., 2017. Cu (II) salen complex with propylene linkage: An efficient catalyst in the formation of CX bonds (X= N, O, S) and biological investigations. *Journal of Molecular Structure*. 1130, 122–127.
- Barros, L., Baptista, P., Ferreira, I.C., 2007. Effect of *Lactarius piperatus* fruiting body maturity stage on antioxidant activity measured by several biochemical assays. *Food and Chemical Toxicology*. 45 (9), 1731–1737.
- Bayda, S., Adeel, M., Tuccinardi, T., Cordani, M., Rizzolio, F., 2019. The History of Nanoscience and Nanotechnology: From Chemical–Physical Applications to Nanomedicine. The history of nanoscience and nanotechnology: from chemical–physical applications to nanomedicine. 25 (1), 112.
- Chen, L.Q., Fang, L.i., Ling, J., Ding, C.Z., Kang, B., Huang, C.Z., 2015. Nanotoxicity of Silver Nanoparticles to Red Blood Cells: Size Dependent Adsorption, Uptake, and Hemolytic Activity. Nanotoxicity of silver nanoparticles to red blood cells: size dependent adsorption, uptake, and hemolytic activity. 28 (3), 501–509.
- Dawadi, S., Katuwal, S., Gupta, A., Lamichhane, U., Thapa, R., Jaisi, S., Lamichhane, G., Bhattarai, D.P., Parajuli, N., Karimi-Maleh, H., 2021. Current Research on Silver Nanoparticles: Synthesis, Characterization, and Applications. *Journal of Nanomaterials* 2021, 1–23.
- Faisal, S., Jan, H., Shah, S.A., Shah, S., Khan, A., Akbar, M.T., Rizwan, M., Jan, F., Wajidullah, Akhtar, N., Khattak, A., Syed, S., 2021. Green Synthesis of Zinc Oxide (ZnO) Nanoparticles Using Aqueous Fruit Extracts of *Myristica fragrans*: Their Characterizations and Biological and Environmental Applications. Green synthesis of zinc oxide (ZnO) nanoparticles using aqueous fruit extracts of *Myristica fragrans*: their characterizations and biological and environmental applications. 6 (14), 9709–9722.
- Fan, T., Wang, J., Yuan, W., et al., 2010. Purification and characterization of hatching enzyme from brine shrimp *Artemia salina*. 42 (2), 165–171.
- Farnsworth, N.R., 1966. Biological and phytochemical screening of plants. *Journal of pharmaceutical sciences*. 55 (3), 225–276.
- Fierascu, R.C., Temocico, G., Fierascu, I., Ortan, A., Babeanu, N.E., 2020. *Fragaria Genus: Chemical Composition and Biological Activities*. *Fragaria genus: Chemical composition and biological activities*. 25 (3), 498.
- Fitri, N., Fitriastuti, D., 2019. Comparison between maceration and microwave extraction techniques of strawberry fruit (*fragaria sp*) and antioxidant activity test. *IOP Conf. Ser.: Mater. Sci. Eng.* 523 (1), 012024.
- Garcia-Viguera, C., P. Zafrilla, F. A. J. P. A. I. J. o. P. C. Tomás-Barberán, et al., 1998. The use of acetone as an extraction solvent for anthocyanins from strawberry fruit. 9 (6) 274–277.
- Guan, Q., Xia, C., Li, W., 2019. Bio-friendly controllable synthesis of silver nanoparticles and their enhanced antibacterial property. Bio-friendly controllable synthesis of silver nanoparticles and their enhanced antibacterial property. 327, 196–202.
- Hong, S.J., Yeoung, Y.R., H., L., J., F., s., Eum, et al., 2018. Phytochemical composition of everbearing strawberries and storage quality of strawberry fruit treated by precooling. 27 (6), 1675–1683.
- Jemal, K., Sandeep, B.V., Pola, S., 2017. Synthesis, Characterization, and Evaluation of the Antibacterial Activity of *Allophylus serratus* Leaf and Leaf Derived Callus Extracts Mediated Silver Nanoparticles. *Journal of Nanomaterials* 2017, 1–11.
- Karaaslan, N.M., Yaman, M., 2017. Anthocyanin profile of strawberry fruit as affected by extraction conditions. Anthocyanin profile of strawberry fruit as affected by extraction conditions. 20 (sup3), S2313, S2322.
- Kargozar, S., Mozafari, M., 2018. Nanotechnology and Nanomedicine: Start small, think big. *Nanotechnology and Nanomedicine: Start small, think big*. 5 (7), 15492–15500.
- Khan, I., Saeed, K., Khan, I., 2019. Nanoparticles: Properties, applications and toxicities. *Nanoparticles: Properties, applications and toxicities*. 12 (7), 908–931.
- Kyrychenko, A., Korsun, O.M., Gubin, I.I., Kovalenko, S.M., Kalugin, O.N., 2015. Atomistic simulations of coating of silver nanoparticles with poly (vinylpyrrolidone) oligomers: Effect of oligomer chain length. *The Journal of Physical Chemistry C*. 119 (14), 7888–7899.
- Li, X., Wang, L.u., Fan, Y., Feng, Q., Cui, F.-Z., 2012. Biocompatibility and Toxicity of Nanoparticles and Nanotubes. *Journal of Nanomaterials* 2012, 1–19.
- Malagoli, D., 2007. A full-length protocol to test hemolytic activity of palytoxin on human erythrocytes. *Invertebrate Survival Journal*. 4 (2), 92–94.
- Markham, K., 1988. Cara mengidentifikasi flavonoid. *Itb, Bandung*, pp. 1–3.
- Mitchell, M.J., Billingsley, M.M., Haley, R.M., Wechsler, M.E., Peppas, N.A., Langer, R., 2021. Engineering precision nanoparticles for drug delivery. *Engineering precision nanoparticles for drug delivery*. 20 (2), 101–124.
- Moldovan, B., David, L., Achim, M., Clichici, S., Filip, G.A., 2016. A green approach to phytomediated synthesis of silver nanoparticles using *Sambucus nigra* L. fruits extract and their antioxidant activity. *Journal of Molecular Liquids* 221, 271–278.
- Mughal, B., Zaidi, S.Z.J., Zhang, X., Hassan, S.U., 2021. Biogenic nanoparticles. Synthesis, characterisation and applications. 11 (6), 2598.
- Mukherjee, P., Ahmad, A., Mandal, D., Senapati, S., Sainkar, S.R., Khan, M.I., Parishcha, R., Ajaykumar, P.V., Alam, M., Kumar, R., Sastry, M., 2001. Fungus-mediated synthesis of silver nanoparticles and their immobilization in the mycelial matrix: a novel biological approach to nanoparticle synthesis. *Nano letters*. 1 (10), 515–519.
- Murdock, R.C., Braydich-Stolle, L., Schrand, A.M., Schlager, J.J., Hussain, S.M., 2008. Characterization of Nanomaterial Dispersion in Solution Prior to In Vitro Exposure Using Dynamic Light Scattering Technique. Characterization of nanomaterial dispersion in solution prior to in vitro exposure using dynamic light scattering technique. 101 (2), 239–253.
- Nagesh, M.R., Kumar, N., Khan, J.M., et al., 2022. Green synthesis and pharmacological application of silver nanoparticles using ethanolic extract of *Salacia chinensis* L. *Journal of King Saud University-Science*. 102284.
- Pokrajac, L., Abbas, A., Chrzanowski, W., et al., 2021. Nanotechnology for a sustainable future: Addressing global challenges with the international network4sustainable nanotechnology. *ACS Publications*.
- Pokrajac, L., Abbas, A., Chrzanowski, W., et al., 2022. Nanotechnology for a Sustainable Future: Addressing Global Challenges with the International Network4Sustainable. *Nanotechnology*. 22–03, 15.
- Priyadarshini, S., Gopinath, V., Priyadarshini, N.M., et al., 2013. Synthesis of anisotropic silver nanoparticles using novel strain. *Bacillus flexus* and its biomedical application. 102, 232–237.
- Roy, K., Sarkar, C., Ghosh, C.J.A.N., 2015. Plant-mediated synthesis of silver nanoparticles using parsley (*Petroselinum crispum*) leaf extract: spectral analysis of the particles and antibacterial study. 5 (8), 945–951.
- Schneidman-Duhovny, D., Inbar, Y., Nussinov, R., et al., 2005. PatchDock and SymmDock: servers for rigid and symmetric docking. *Nucleic acids research*. 33 (suppl_2), W363, W367.
- Shanmuganathan, R., MubarakAli, D., Prabakar, D., et al., 2018. An enhancement of antimicrobial efficacy of biogenic and ceftriaxone-conjugated silver nanoparticles: green approach. 25 (11), 10362–10370.
- Sharma, D., Kanchi, S., K., J., A., j., o., c., Bisetty,, 2019. Biogenic synthesis of nanoparticles: a review. 12 (8), 3576–3600.

- Tarafdar, J., Sharma, S., R., J., A., J., o., B., Raliya,, 2013. Nanotechnology: Interdisciplinary science of applications, 12.
- Umoren, S.A., Nzila, A.M., Sankaran, S., et al., 2017. Green synthesis, characterization and antibacterial activities of silver nanoparticles from strawberry fruit extract. Polish Journal of Chemical Technology. 19 (4).
- Unal, I.S., Demirbas, A., Onal, I., et al., 2020. One step preparation of stable gold nanoparticle using red cabbage extracts under UV light and its catalytic activity. 204, 111800.
- Vinodhini, S., Vithiya, B.S.M., Prasad, T.A.A., 2022. Green synthesis of silver nanoparticles by employing the *Allium fistulosum*, *Tabernaemontana* divaricate and *Basella alba* leaf extracts for antimicrobial applications. Journal of King Saud University-Science. 34, (4) 101939.
- Warad, I., Azam, M., Al-Resayes, S.I., et al., 2014. Structural studies on Cd (II) complexes incorporating di-2-pyridyl ligand and the X-ray crystal structure of the chloroform solvated DPMNPH/CdI₂ complex. Inorganic Chemistry Communications. 43, 155–161.
- Zhang, D., Ma, X.-L., Gu, Y., et al., 2020. Green synthesis of metallic nanoparticles and their potential applications to treat cancer. 8, 799.